

## ORIGINAL ARTICLE

# Numerical Simulation of flow in bottom outlet of Narmashir dam for Calculating of Hydrodynamic forces

Mehdi Nezhad Naderi<sup>\*1</sup>, Ehsanallah Hadipour<sup>2</sup>

<sup>\*1</sup> Department of Civil Engineering, Tonekabon Branch, Islamic Azad University, Tonekabon, Iran,  
Email: Mehdi2930@yahoo.com

<sup>2</sup> Department of Civil Engineering, Tonekabon Branch, Islamic Azad University, Tonekabon, Iran.

### ABSTRACT

The bottom outlets are used to transfer water from the lake to the dam downstream. Performance analysis includes a discharge conduit, and outlet valve has a special sensitivity to them. In this Study is evaluated the pressure distribution around the outlet channels and the calculating of hydrodynamic forces was carried out. Numerical Solution carried out by Fluent software that is based on finite volume method. Then physical model results were compared with results of numerical models. Velocity and pressure values obtained from the numerical values of the pressure on the valve per valve opening of 30%, 50% and 80%. The results show that the pressure values obtained from the numerical model and previous studies follow a similar pattern. For greater amount of percentage of gate opening the pressure exerted on the bottom and top of the valve opening is reduced. According to the results of previous studies and numerical model, always difference of pressure exerted on the bottom and top of the valve is caused down pull force.

**Keywords:** Bottom outlets, hydrodynamic forces, slide valve, physical model, Fluent.

Received 13/07/2013 Accepted 01/10/2013

©2013 AE LS, INDIA

### INTRODUCTION

Accurate calculation of the force and velocity of water in the canal tunnel on the costs of construction, repair and reconstruction will affect them. When the valve is placed in the channel width, a force is formed in below or top of valve because the flow through the valve and hydrostatic pressure entered on the lower edge. The pressure force, valve weight and friction force determine the force required for down pulling and upper pulling of valve. For valves located inside the tunnels, down pulling force or upper pulling force also strongly influenced by the geometry of the valve and intensity of flow from below and top of the valve. Sadeghi Pour et al., [1] were examined model of the bottom outlet of Maroondam and the results were compared with the aerodynamic model. The pressures were measured to calculate the hydrodynamic forces exerted on the valve. Model results are very well consistent with results of aerodynamic model by [1]. [2] are paid to the numerical model of the bottom outlet for calculation of the hydrodynamic down pulling forces exerted on the valve. [3] are paid to the numerical simulation of flow from bottom outlet of Shahid Abbas pourdam. They compared the obtained values of lower jet velocity and the exerted force on the valve by software with obtained values by empirical relationship. In this study the simulation of flow was carried out without aeration duct. Velocity field and pressure loads were calculated and compared with the results of laboratory model of bottom outlet of Narmashirdam. Vertical forces acting on the valve are calculated by the pressure distribution under the valve surface. Based on empirical governing equations of flow in valve in the bottom tunnel which is provided by [4], down pull force is calculated from on difference between upper and lower forces on surfaces of the valve as follows [4]:

$$F_d = (K_t - K_b) B \cdot d \cdot \rho \frac{V_j^2}{2} \quad (1)$$

$F_d$  is down pull force,  $K_t$  is coefficient force in top of the valve,  $K_b$  is coefficient force in below the valve and  $V_j$  jet velocity.  $K_b$  and  $K_t$  are coefficients based on experimental plots provided by [4] and geometrical factors, the percentage of valve opening and valve sealing [2]. Figure 1 shows values of the forces and the jet velocity per the percentage of opening the valve [4].

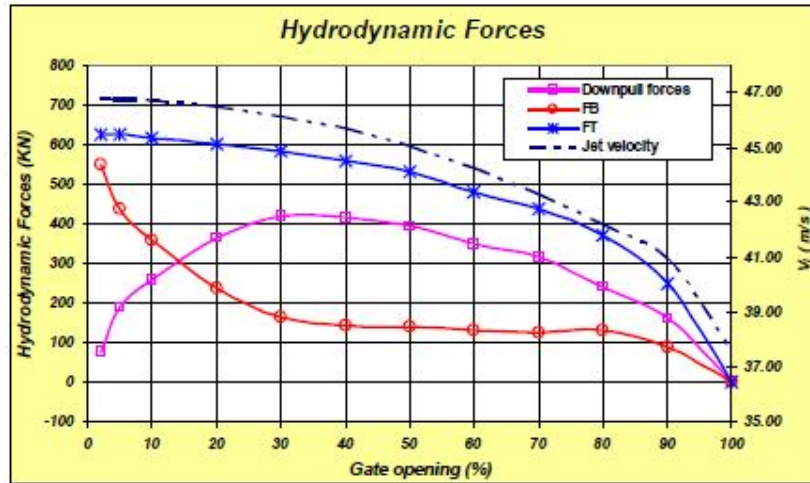


Figure 1: The values of the forces and jet velocity per the percentage of gate opening[4].

**MATERIALS AND METHODS**

Model of outlet channel of Narmashirdam (with 1354.63 m floor entrance level above sea level) include the bell shape inlet, an emergency valve, a service valve and part of the duct downstream. This model was constructed according to the plans offered by the project employer at a scale 1:15. In this model, in order to coping with adverse effects of pressure reducing on downstream valve, an aerator tube is provided in downstream of service valve with a diameter of 6 cm and a height of 40 cm. an aerator tube is provided in downstream of the emergency valve with a diameter of 13 mm and a height of 25 cm. Certainly this model did not apply for simulation of the air movement into the prototype model but air velocity measurement in the pipe can be guidelines on air velocity in the air tunnel of prototype model [1].

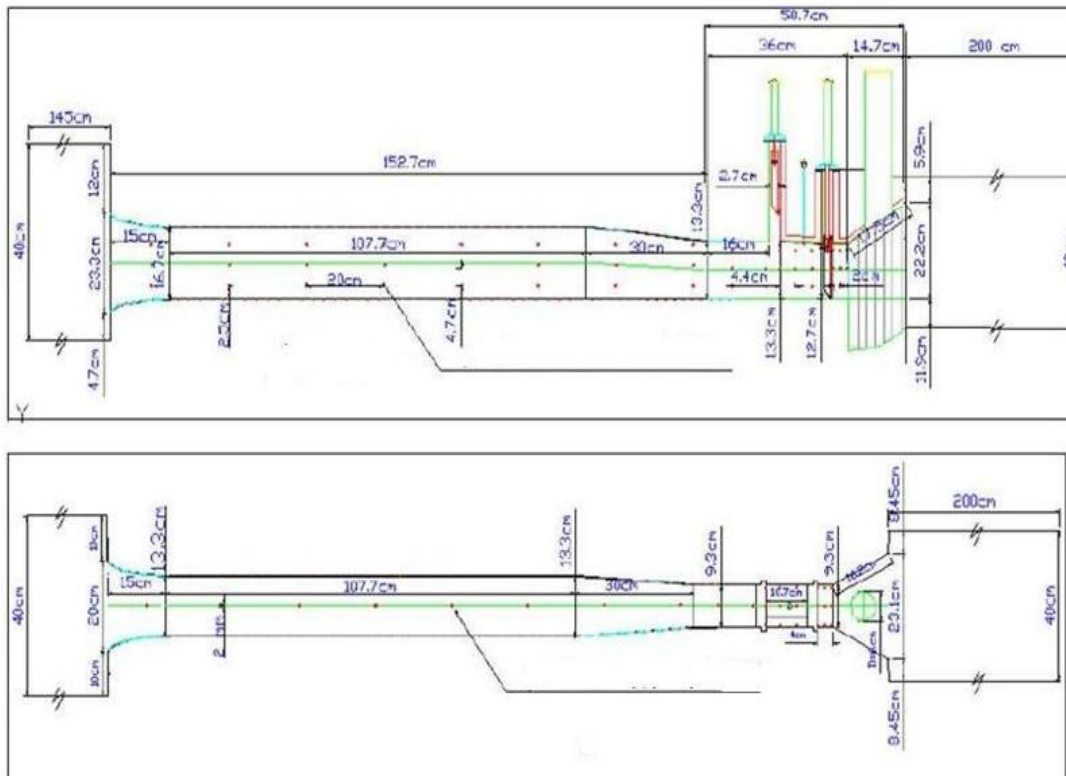


Figure 2 - Geometry ducts, valves and ... in physical model of Narmashir dam (Sadeghi Pour et al., 2008).

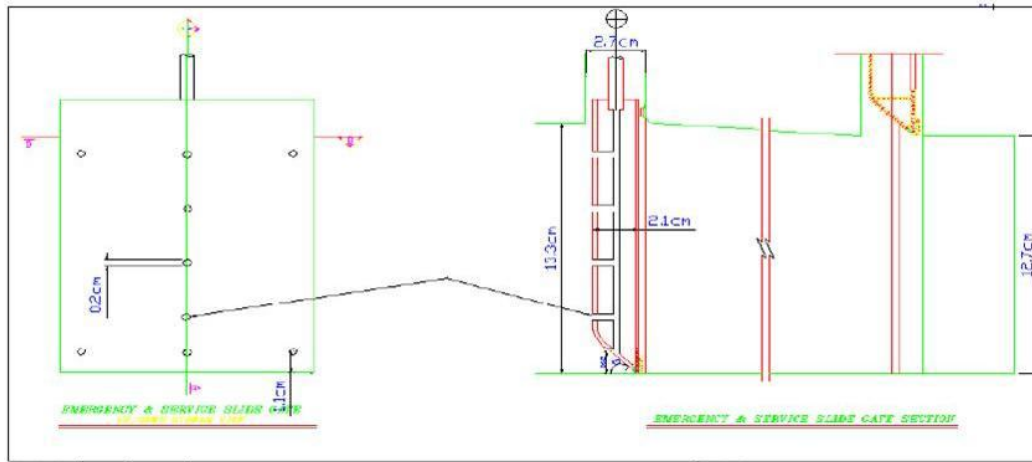


Figure 3- Geometry ducts, valves and... in physical model of Narmashir (Sadeghi Pour et al., 2008).

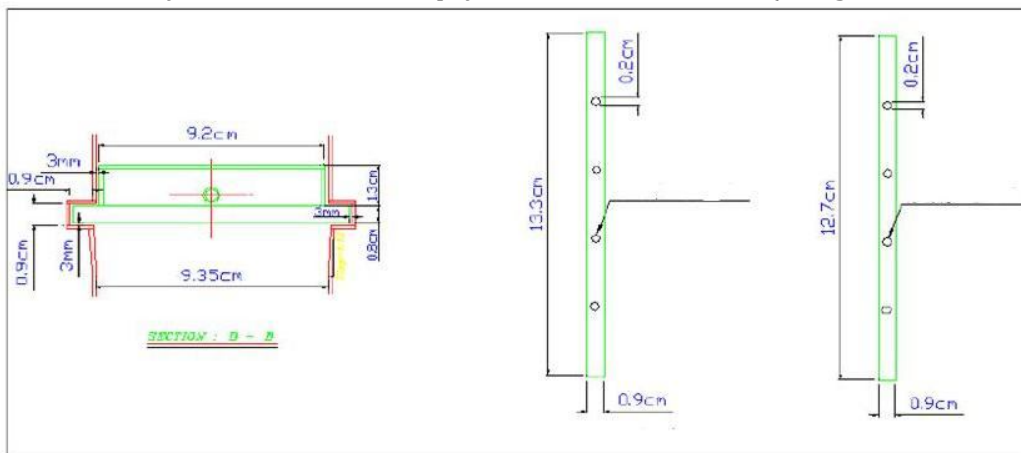


Figure4: Geometry ducts, valves and... in physical model of Narmashir (Sadeghi Pour et al., 2008).

Table1: Horizontal and vertical forces exerted on the service valve in normal head (Sadeghi Pour et al., 2008).

Service gate opening	$P/\gamma$	$P/\gamma$	$A_{top}$	$A_{bottom}$	$F_t(KN)$	$F_b(KN)$	$F_{dp}(KN)$	$F_h(KN)$
90	258.4	549.4	0.42	0.448	108.5	241.5	132.9-	1081
80	273.11	466.9	0.42	0.448	114.7	205.2	90.5-	1213
70	371.1	427.9	0.42	0.448	156.1	188.1	31.9-	1317.3
60	449.69	378.4	0.42	0.448	188.9	166.3	22.6	1619
50	493.84	363.4	0.42	0.448	207.4	159.7	47.7	1765
40	571.82	388.9	0.42	0.448	240.2	170.9	69.2	1843
30	608.61	457.9	0.42	0.448	255.6	201.2	54.4	2020.9
20	661.559	561.4	0.42	0.448	277.9	246.7	31.1	2134.1
10	677.77	732.4	0.42	0.448	284.9	321.9	37.2-	2334.4
5	705.33	838.9	0.42	0.448	296.4	368.7	-72.3	2404
2	726.33	910.1	0.42	0.448	305.1	400	-94.92	2410.9

In this study, flow is steady with two-dimensional turbulence form. To model of the velocity and pressure fluctuations is the integrated from the Navier Stokes equation at time. Integration of Navier Stokes equations at time is known Reynolds equations [5]. Turbulence model equations are two equation models k-ε (Standard) that have be averaged in depth [6]. ε equation is as one of the main sources of the limitations of accuracy of the standard version of the k-ε model and the Reynolds stress model. It is interesting that k-ε model includes a correction term that is dependent to strain with c13 constant in the ε equation of RNG model [7] WillCox provided turbulence equations of k-ω (standard) model [8].

$$\frac{\partial u}{\partial x} + \frac{\partial v}{\partial y} + \frac{\partial w}{\partial z} = 0 \quad (2)$$

$$\frac{\partial \rho u}{\partial t} + \frac{\partial \rho u u}{\partial x} + \frac{\partial \rho u v}{\partial y} + \frac{\partial \rho u w}{\partial z} - \rho f_c v = -\frac{\partial P}{\partial x} + \frac{\partial \tau_{xx}}{\partial x} + \frac{\partial \tau_{xy}}{\partial y} + \frac{\partial \tau_{xz}}{\partial z} \quad (3)$$

$$\frac{\partial \rho v}{\partial t} + \frac{\partial \rho u v}{\partial x} + \frac{\partial \rho v v}{\partial y} + \frac{\partial \rho v w}{\partial z} + \rho f_c u = -\frac{\partial P}{\partial y} + \frac{\partial \tau_{yx}}{\partial x} + \frac{\partial \tau_{yy}}{\partial y} + \frac{\partial \tau_{yz}}{\partial z} \quad (4)$$

$$\frac{\partial \rho w}{\partial t} + \frac{\partial \rho u w}{\partial x} + \frac{\partial \rho v w}{\partial y} + \frac{\partial \rho w w}{\partial z} = -\frac{\partial P}{\partial z} + \frac{\partial \tau_{zx}}{\partial x} + \frac{\partial \tau_{zy}}{\partial y} + \frac{\partial \tau_{zz}}{\partial z} - \rho g \quad (5)$$

Known two-equation model of k-ε (Standard) are presented for averaged form in depth as follows [6] :

$$\frac{\partial h k}{\partial t} + \frac{\partial U_j h k}{\partial x_j} = \frac{\partial}{\partial x_j} \left[ \left( v + \frac{v_t}{\sigma_k} \right) h \frac{\partial k}{\partial x} \right] + h P_k + h P_{kv} - h \varepsilon \quad (6)$$

$$\frac{\partial h \varepsilon}{\partial t} + \frac{\partial U_j h \varepsilon}{\partial x_j} = \frac{\partial}{\partial x_j} \left[ \left( v + \frac{v_t}{\sigma_\varepsilon} \right) h \frac{\partial \varepsilon}{\partial x} \right] + h c_{1\varepsilon} \frac{\varepsilon}{k} P_k + h P_{\varepsilon v} - h c_{2\varepsilon} \frac{\varepsilon^2}{k} \quad (7)$$

$$v_t = c_\mu \frac{k^2}{\varepsilon}, P_k = 2v_t S_{ij} \cdot S_{ij} \quad (8)$$

$$P_{kv} = c_k \frac{k^2}{\varepsilon}, c_k = \frac{1}{c_f^{1/2}}, P_{\varepsilon v} = c_\varepsilon \frac{u_f^4}{h^2}, c_\varepsilon = \frac{1}{\sqrt{e_* \sigma_t}} \frac{c_{2\varepsilon} c_\mu^{1/2}}{c_f^{3/4}}, c_f = \frac{u_f^2}{u^2 + v^2 + w^2} = \frac{n^2 g}{h^{1/3}} \quad (9)$$

$$c_\mu = 0.09, c_{\varepsilon 1} = 1.44, c_{\varepsilon 2} = 1.92, \sigma_k = 1.0, \sigma_\varepsilon = 1.31$$

$P_{kv}$  and  $P_{kv}$  are production terms as result of non-uniform distribution velocity in depth that is stronger near-bed.  $P_k$  is production term of turbulent kinetic energy averaged in depth as result of velocity gradients in the plan.  $v_t$  is the vortex viscosity. Turbulence model is used for calculation of lateral flow into one channel and is achieved much better results in comparison with  $v_t$  for fixed parameters of rotational flow [9].  $c_f$  is the bed friction coefficient.  $\sigma_t$  is Schmidt number that shows relationship between turbulence viscosity and turbulent diffusion coefficient according to the following equation:

$$\varepsilon_d = \frac{v_t}{\sigma_t} \quad (10)$$

Amount of  $\sigma_t$  is considered 0.5 [10]. Although values of  $\sigma_t$  are 0.5 to 2 in variable references [11].  $e_*$  is coefficient that gives turbulence diffusion coefficient in depth by following equation [10].

$$\varepsilon_d = e_* h u_f \quad (11)$$

Direct measurement of color broadcasting in the fixed-width channels offers 0.15 for  $e_*$ . Although Keller and Rodi achieved better solutions for the velocity and stress within the composite channels [10]. On the other hand Biglari and Sturm have been assumed  $e_*$  equaled to 0.3 to get the better answer within the composite channels [12]. MCGurik and Rodi have considered  $\frac{1}{\sqrt{e_* \sigma_t}}$  equaled to 3.6 [9]. In  $\varepsilon$  equation of

RNG model includes a correction term  $c_{\varepsilon 1}$  that is constant strain-dependent[7]. For k-ε (RNG), we have:

$$\frac{\partial h \varepsilon}{\partial t} + \frac{\partial U_j h \varepsilon}{\partial x_j} = \frac{\partial}{\partial x_j} \left[ \left( v + \frac{v_t}{\sigma_\varepsilon} \right) h \frac{\partial \varepsilon}{\partial x} \right] + h c_{1\varepsilon}^* \frac{\varepsilon}{k} P_k + h P_{\varepsilon v} - h c_{2\varepsilon} \frac{\varepsilon^2}{k} \quad (12)$$

$$c_{\mu} = 0.0845, c_{1\varepsilon}^* = c_{1\varepsilon} - \frac{\eta(1 - \frac{\eta}{\eta_0})}{1 + \beta\eta^3}, c_{1\varepsilon} = 1.68, \sigma_k = 1.39, \beta = 0.012, c_{1\varepsilon} = 1.42, \quad (13)$$

$$\eta = (2E_{ij} \cdot E_{ij})^{1/2} \frac{k}{\varepsilon}, \eta_0 = 4.377$$

Only constant  $\beta$  is adjustable, high levels of turbulent data are obtained near-wall. All other constants are calculated explicitly as part of the RNG process.

$$\frac{\partial hk}{\partial t} + \frac{\partial U_j hk}{\partial x_j} = \frac{\partial}{\partial x_j} [(v + \frac{v_t}{\sigma_k}) h \frac{\partial k}{\partial x}] + P_k + P_b - h\varepsilon \quad (14)$$

$$\frac{\partial h\varepsilon}{\partial t} + \frac{\partial U_j h\varepsilon}{\partial x_j} = \frac{\partial}{\partial x_j} [(v + \frac{v_t}{\sigma\varepsilon}) h \frac{\partial \varepsilon}{\partial x}] + hc_{1\varepsilon} \frac{\varepsilon}{k} P_k + hc_1 S_\varepsilon - hc_2 \frac{\varepsilon^2}{k + \sqrt{v\varepsilon}} + S_\varepsilon \quad (15)$$

$$c_1 = \text{Max}[0.43, \frac{\eta}{\eta + s}], \eta = s \frac{k}{\varepsilon}, s = \sqrt{2s_{ij}s_{ij}}, \mu_t = hc_\mu \frac{k^2}{\varepsilon}, P_k = -\rho u_i u_j \frac{\partial u_j}{\partial x_i},$$

$$P_k = \mu_t s^2, P_b = \beta g_i \frac{\mu_t}{Pr_t} \frac{\partial T}{\partial x_i}, \mu_t = \rho c_\mu \frac{k^2}{\varepsilon}, c_\mu = \frac{1}{A_0 + A_s \frac{KU^*}{\varepsilon}}, U^* = \sqrt{s_{ij}s_{ij} + \overline{\Omega_{ij}\Omega_{ij}}}, \quad (16)$$

$$\overline{\Omega_{ij}} = \Omega_{ij} - \varepsilon_{ijk} \omega_k, A_0 = 4.04, A_s = \sqrt{6} \cos \Phi, \Phi = \frac{1}{3} \cos^{-1}(\sqrt{6}\omega), \omega = \frac{s_{ij}s_{jk}s_{ki}}{\tilde{s}^3}, \tilde{s} = \sqrt{s_{ij}s_{ij}},$$

$$s_{ij} = \frac{1}{2} (\frac{\partial u_j}{\partial x_i} + \frac{\partial u_i}{\partial x_j}), c_{1\varepsilon} = 1.44, c_2 = 1.9, \sigma_k = 1, \sigma_\varepsilon = 1.2, \beta = -\frac{1}{\rho} (\frac{\partial P}{\partial T}) p, Pr_t = 0.85$$

WillCox, turbulence model k- $\omega$  (standard) equation to be provided as follows [8]:

$$\frac{\partial k}{\partial t} + U_j \frac{\partial k}{\partial x_j} = \tau_{ij} \frac{\partial U_i}{\partial x_j} - \beta^* k\omega + \frac{\partial}{\partial x_j} [(v + \sigma^* v_T) \frac{\partial k}{\partial x_j}] \quad (17)$$

$$\frac{\partial \omega}{\partial t} + U_j \frac{\partial \omega}{\partial x_j} = \alpha \frac{\omega}{k} \tau_{ij} \frac{\partial U_i}{\partial x_j} - \beta \omega^2 k\omega + \frac{\partial}{\partial x_j} [(v + \sigma v_T) \frac{\partial \omega}{\partial x_j}] \quad (18)$$

$$v_t = \frac{k}{\omega}, \alpha = \frac{5}{9}, \beta = \frac{3}{40}, \beta^* = \frac{9}{100}, \sigma = \frac{1}{2}, \varepsilon = \beta^* \omega k$$

The values of the physical properties of water are considered 998.2, 0.001003, 4182 and 0.6, respectively, for density, viscosity, heat capacity and thermal conductivity. Solutions of all governing equations are subject to assignment of variables correctly in the boundary nodes. In steady state problems required only boundary condition but in unsteady state problems is required the initial conditions for all nodes in the network. Common boundary conditions in hydraulic issues include [13]:

A- Inlet boundary condition: numerical models can fit the model by means of the various boundary conditions such as velocity, mass flow, etc. For example, in modeling of flow inside a closed or open channel can be used velocity inlet as input boundary condition. B- The outlet boundary condition is considered pressure outlet equals the atmospheric pressure. If the output is chosen at a far distance from geometric constraints, and no change in direction of flow then the flow state is developed full. Using this model is caused the output surface is perpendicular to the flow and gradient is zero in the perpendicular direction on the output surface [13]. C - Wall boundary condition: the wall boundary condition is used to limit the area of between fluid and solid. The model is ready for simulation by Solutions set and defining the model. The following steps show the simulation process [14]: selection methods of discretization equation: In this paper first order upstream difference method is used for discretization of momentum, k,  $\varepsilon$  and  $\omega$  equations and the standard method is used to find the pressure. Selection methods of the relation

velocity - Pressure: this step is only be studied segregated. In this paper is used from SIMPLE method for velocity - pressure coupling. Determine the discount factors: the discount factor values are used for control of calculated variables in the each iteration. In this paper, the default values 0.3, 1, 0.7, 0.8, 0.8 and 1 is used respectively for the pressure, density, momentum,  $k$ ,  $\epsilon$  and turbulent viscosity. In this paper, the initial values of the relative pressure is considered zero And the initial values of velocity components close to the average values presented in the input stream. By completing the steps in the numerical model, we can start the introduced process of problem by defining of repeat process. The frequency of reporting of results can be introduced before computing the numerical model. During solution process can be seen convergence of solution by the control of residues, integral of surface, statistics and values of the force. After finishing solution the computation of the unknown quantities and the results can be calculated at any point of the field and can be displayed by vector in the form, contour and profile [14]. In this paper for solution of flow is usually introduced initial number repeat 1000 with report of every step of the calculation that conditions for convergence of the unknown parameters were satisfied after 300 to 350 iterations. Gambit software version 2.3.16 is used to generate the channel geometry and meshing[15]. Model of the network is used Quad element and the types of Map and Pave for pages and Hex elements and types of Map of Cooper for volumes. Inlet and outlet and wall boundary conditions and symmetry were introduced in the software.

### RESULTS AND DISCUSSION

The bottom outlets are used to transfer water from the lake to the dam downstream. In this Study is evaluated the pressure distribution around the outlet channels and the calculating of hydrodynamic forces was carried out. Numerical Solution carried out by Fluent software that is based on finite volume method. Then physical model results were compared with results of numerical models. Velocity and pressure values obtained from the numerical values of the pressure on the valve per valve opening of 30%,50% and 80%. The results show that the pressure values obtained from the numerical model and previous studies follow a similar pattern. According to the results of [4], Figure 1, always difference of pressure exerted on the bottom and top of the valve is caused downpull force.

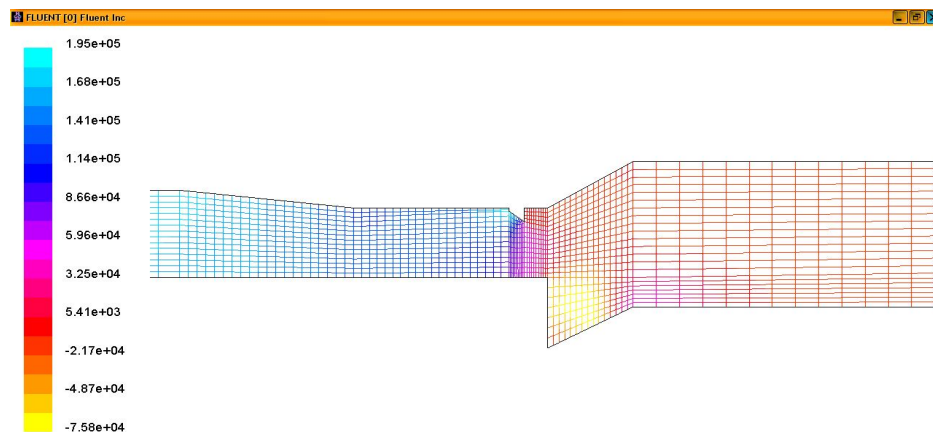


Figure 5 - The pressure contour according to Pascal, percentage of gate opening = 80% and using  $k-\epsilon$  turbulence model

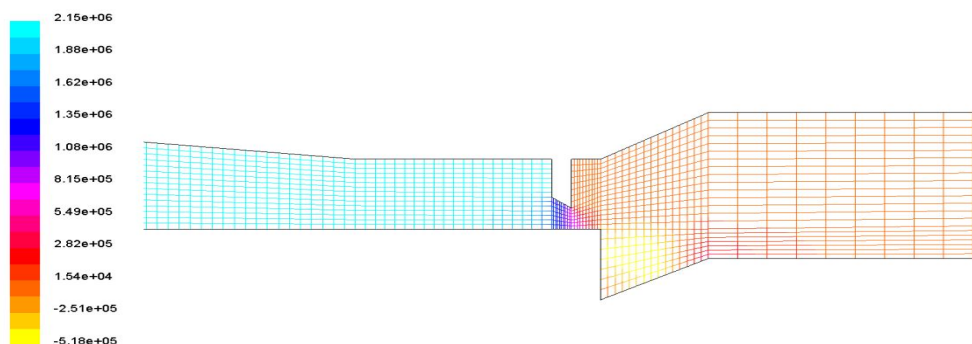


Figure 6 - The pressure contour according to Pascal, percentage of gate opening = 30% and using  $k-\epsilon$  turbulence model

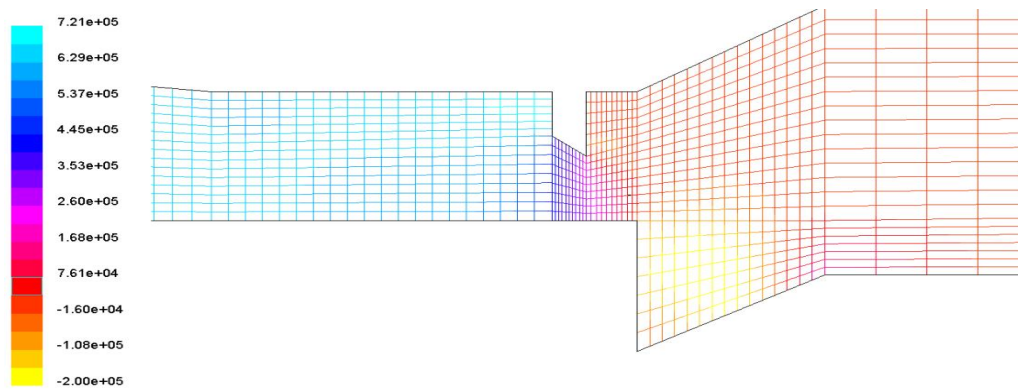


Figure 7 - The pressure contour according to Pascal, percentage of gate opening = 50% and using k-  $\epsilon$  turbulence model

## CONCLUSION

The bottom outlet structures set up to transfer water from lack of dam to discharge point at downstream of dam. This study aimed to calculate the pressure and velocity of flow in the valve at different percentage of gate opening. In this paper, the governing equations of flow are in two-dimensional. Governing equations of flow in physical model of the bottom outlet of Narmashir dam were solved by using of appropriate k-  $\epsilon$  turbulence model. The flow pattern and turbulence were measured. Velocity and pressure values obtained from the numerical values of the pressure on the valve per valve opening of 30%, 50% and 80%. The results show that the pressure values obtained from the numerical model, results by [4], Figure1, and the results of [1], Table 1, follow a similar pattern. For greater amount of percentage of gate opening the pressure exerted on the bottom and top of the valve opening is reduced. For the percentage of gate opening more than 70% and less than 10 % the results obtained from [4], Figure 1, are different with results obtained from [1], Table 1. According to the results of [4], Figure 1, always difference of pressure exerted on the bottom and top of the valve is caused downpull force.

## REFERENCES

1. Hosseini, S. A., Sanei, M., Parehkar, M., Habibi, M., Davoodi, M. M. and Ghafoori, A. (2008). Hydraulic model of bottom outlet of Narmashir dam. Soil Conservation and Watershed Management Research Institute, Tehran, Iran.
2. SabbaghYazdi, S. R. and Abolghasemi, M. (2003). Numerical analysis of hydrodynamic downpull forces exerted on the valve slide. National Conference of hydraulic power plants, in Tehran, Iran.
3. BaniSoltan, S., Pirzadeh, B. And Kaviyanpour, M. R. (2010). Numerical modeling of bottom outlet of ShahidAbbaspour dam byFluent software", Fifth National Congress on Civil Engineering, Mashhad, Iran.
4. EduardNaudascher, F. ASCE, Palepu, V. Rao, Andreas Richter, Patricio Vargas and Georg Wonik, (1986). "PREDICTION AND CONTROL OF DOWNPULLON TUNNEL GATES. Journal of Hydraulic Engineering, Vol 112; No 5;1986
5. Reynolds, O. (1984). On the Dynamical Theory of Incompressible Viscous Fluids and the Determination of the Criterion, Phil. Trans. Roy. Soc. London, 1986, 123-161
6. Rastogi, A. K., and Rodi, W. (1978). Prediction of Heat and Mass Transfer in Open Channels. Journal of Hydraulics Division, ASCE, 104(3), 397- 420.
7. Yakhot, V., Orszag, S.A., Thangam, S., Gatski, T. B., and speziale, C. G. (1992). Development of turbulence models for shear flows by a double expansion technique, Physics of Fluids A, Vol. 4, No. 7, pp1510-1520.
8. Wilcox, D. C. (1988). Re-assessment of the scale-determining equation for advanced turbulence models, AIAA Journal, vol. 26, pp. 1414- 1421
9. McGurik, J. J., and Rodi, W. (1978). A Depth- Averaged Mathematical Model for the Near Fluid of SideDischarge into open- channel Flow. Journal of Fluid Mechanics, 864, 761-781.
10. Keller, R. J., and Rodi, W. (1988). Prediction of Flow Characteristics in Main Channel/Floodplain Flows", Journal of Hydraulic Research, IAHR, 26(4), 425- 441
11. Gibson, M. M., and Lauder, B. E. (1978). Ground Effects on Pressure Fluctuations in the Atmospheric Boundary Layers. Journal of Fluid Mechanics, 86, 491-511.
12. Biglari, B., and Sturm, T. W. (1998). "Numerical Modeling of Flow Around the Bridge Abutments in Compound Channel. Journal of Hydraulic Engineering, ASCE, 124(2), 156-163.
13. Soltani, M. V. and RahimiAsl,R., (2003). Computational Fluid Dynamics by Fluent Software, Tehran, Tarrah issues.
14. Versteeg, H. K. and Malalasekera, W. (1995). An Introduction to Computational Fluid Dynamics.
15. GAMBIT 2.2 User's Guide, September (2004).

### How to cite this article

Mehdi Nezhad Naderi, Ehsanallah Hadipour. Numerical Simulation of flow in bottom outlet of Narmashir dam for Calculating of Hydrodynamic forces. Bull. Env. Pharmacol. Life Sci, Vol 2 (11) October 2013: 87-93